Train Localization with Particle Filter and Magnetic Field Measurements

Benjamin Siebler, Oliver Heirich and Stephan Sand
German Aerospace Center (DLR)
Institute of Communications and Navigation
Wessling, Germany
Email: benjamin.siebler@dlr.de

***Abstract*—In this paper a particle filter for absolute train localization based on magnetic field measurements is proposed. The filter utilizes distortions of the earth magnetic field introduced by ferromagnetic infrastructure components along the railway track. The distortions are characteristic for a certain part of the track network and therefore are a source of position information. The particle filter introduced in this paper incorporates a prior created map of these distortions to estimate the train position. This only requires low-cost passive magnetometers and a simple movement model that accounts for the limited dynamics of a train. The feasibility of the approach is demonstrated in an evaluation with measurements collected on a train driving in a rural area. Overall a position root mean square error below four meters could be achieved, proving that the magnetic field is a viable source of position information that is independent from other localization systems like GNSS.**

I. Introduction

Current railway systems lack the capability to continuously localize the trains in the track network. For safe operation therefore large distances between consecutive trains are required. This is becoming more and more of a problem because the increasing amount of passenger requires a higher density of trains on the tracks. Especially in urban areas this problem cannot be solved by building new infrastructure like tracks because of high costs and limited space. Further, building tracks is time consuming and hence cannot fix the already existing bottlenecks in the near future. One way to handle the increasing amount of passengers that avoids the before mentioned issues of an infrastructure based approach is automation. For automation accurate and reliable train localization is crucial and can be seen as one of the key technologies. The research in this area is focusing on approaches with global navigation satellite systems (GNSS) [1]. GNSS will be a viable localization solution in many scenarios but there are also environments like tunnels, train stations with closed roofs and urban canyons in which GNSS signals are strongly degraded or completely blocked. GNSS signals can also be jammed easily due to the low signal power on the receiver antenna. An alternative to GNSS is the approach that was introduced with the European train control system (ETCS). In the ETCS the train position is determined with a combination of an odometer and radio beacons. The odometer is used to perform dead reckoning in respect to the last radio beacon. The radio beacons are placed in the middle of the track between the rails at known positions. When a train passes a beacon the beacon number is transmitted to the train. With the beacon number the beacon position is obtained from a database. This is used to bound the dead reckoning position error that otherwise would accumulate unlimited over time. While this is in principle a simple system able to provide accurate train positions, it is also expensive to install and to maintain.

In this paper a different approach for train localization is investigated that is completely independent from the before mentioned ones and does not require special infrastructure components. The approach is based on environmental features along the railway track. More precisely, measurements of the magnetic field are utilized to estimate the train position. This is possible because in the vicinity of railway tracks many ferromagnetic infrastructure components like poles, cables and reinforced concrete can be found. These components introduce distortions in the earth magnetic field that have fixed locations. A measurement analysis showed that the distortions are also stable over time. The magnetic field along a railway track therefore contains position information that can be utilized in a localization system. In [2] we showed that the magnetic field has the potential to enable train localization and proposed in [3] an approach for train localization based solely on magnetometers and an inertial measurements unit (IMU).

In the literature the idea of magnetic field localization is also considered for indoor environments. The authors in e.g. [4], [5] use the magnetic field and a particle filter for pedestrian localization. In indoor environments the magnetic distortions are introduced by the metallic structures in the building and magnetic fields generated by electronic devices. In [6] a wheeled robot is localized inside a building with an array of magnetometers and a wheel speed sensor. For roads magnetic localization was investigated in [7]. The authors use a particle filter and a movement model to localize different cars on the road. In this paper we adapt this approach to train localization and propose a particle filter that only requires a map of the magnetic field and magnetometer measurements. This is in contrast to our prior work in [3], where we used a magnetometer to stabilize the position estimate obtained from an inertial navigation system (INS). The INS was used to measure the distance between magnetometer measurements. With this distance information the magnetic field of the last couple of hundred meters of track was calculated and compared to the magnetic field in the prior created map to estimate the train position. This has the advantage that the INS errors can be corrected with a low complexity extended Kalman filter. The downside of the approach is the complicated initialization process of the INS and the requirement for an IMU. The particle filter proposed here is simple to initialize and does not require an IMU or other sensors measuring the kinematic quantities of the train. In addition it is straightforward to incorporate multiple magnetometers into the update step of the filter.

II. Train Localization with Magnetic Field Measurements

A. Train Position in Topological Coordinates

In train localization one is interested in finding the position in respect to the track network. Hence the train position in this paper is defined in topological coordinates. The topological coordinates contain the along-track position s and the track number $\mathcal{I} \in \mathbb{N}$. The along-track position is a real valued variable on the interval $[0, L_{\mathcal{I}}]$ where $L_{\mathcal{I}}$ is the length of track $\mathcal{I}$. In the rest of the paper the focus is on showing the feasibility of the along-track localization and we will assume that the track number is known in advance. This assumptions is reasonable for railways because typically the sequence of tracks $\{\mathcal{I}_j\}_{1:N}$ the train will travel on is known in advance. From that sequence and a map of the track network it is straightforward to combine the different tracks to a virtual track of length $\sum_{j=1}^{N} L_{\mathcal{I}_j}$.

B. Magnetic Field in Railway Environments

Ferromagnetic material in the railway environment introduces distortions in the local earth magnetic field. These distortions are persistent in time and show a strong position dependency. An example for the magnetic field on a $1\,\mathrm{km}$ long railway track segment is shown in Fig. 1. The magnetic field B_n in Fig. 1 is the magnetic field normalized to the undisturbed earth magnetic field. The red and the blue lines are measurements recorded on two runs on the same track segment. The sensitivity axis of the magnetometer was facing downwards during the measurements. In Fig. 1 it is clearly visible that the magnetic field for both runs has a high similarity but it can also be seen that a single magnetic field measurement contains only ambiguous position information. To get a unique position a sequence of measurements must be compared to the map. This can be done either by collecting a batch of measurements like in [3] or iteratively by updating a filter with each measurement as soon it gets available [4], [5], [6], [7]. Both approaches have in common that a prior recorded map containing the magnetic field and the corresponding topological position is required and that the position estimation is based on a comparison of the magnetometer measurements and the map.

III. Particle Filter for Along-track Localization

A. System Model

For along-track position estimation we propose a low dimensional state vector to model the train dynamics. In particular the dynamic state of the train at the discrete time step k is described with the vector

$$\mathbf{x}_k^{\mathrm{D}} = \begin{bmatrix} s_k & \dot{s}_k \end{bmatrix}^T \tag{1}$$

containing the along-track position s_k and the train speed $\dot{s}_k$.

The evaluation is based on a triad of orthogonal magnetometers. The magnetometer axes are facing downwards, parallel

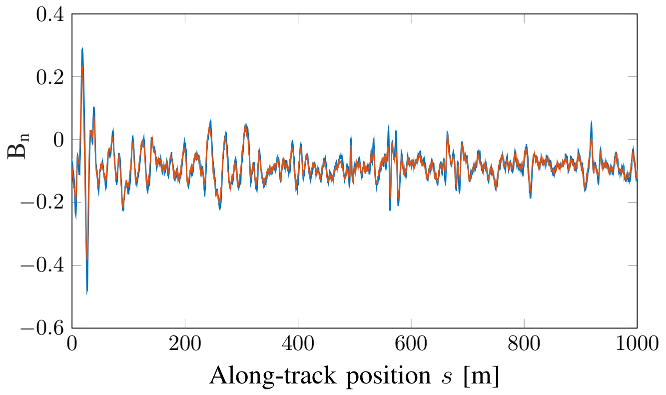

Fig. 1. Example of the magnetic field measured on $1000\,\mathrm{m}$ long track segment.

to the track and perpendicular to the track. The sign of the measurements parallel and perpendicular to the track changes when the orientation of the train on the track changes. In addition to the kinematic state therefore also the orientation is estimated. The orientation can take only two possible values and is modeled as binary variable $\mathcal{O} \in \{-1, +1\}$. The overall state vector estimated in the particle filter is therefore

$$\mathbf{x}_k = \begin{bmatrix} \mathbf{x}_k^{\mathrm{D}} & \mathcal{O}_k \end{bmatrix}^T. \tag{2}$$

The evolution of the dynamic state from the discrete time step $k-1$ to the next time step k is modeled by a white noise acceleration model

$$\mathbf{x}_k^{\mathrm{D}} = \underbrace{\begin{bmatrix} 1 & T \\ 0 & 1 \end{bmatrix}}_{\mathbf{F}^{\mathrm{D}}} \mathbf{x}_{k-1}^{\mathrm{D}} + \mathbf{n}_{k-1} \tag{3}$$

with the process noise $\mathbf{n}_k \sim \mathcal{N}(0, \mathbf{Q})$ and the time increment T. The time discrete process noise covariance is

$$\mathbf{Q} = \begin{bmatrix} \frac{1}{3}T^3 & \frac{1}{2}T^2 \\ \frac{1}{2}T^2 & T \end{bmatrix} q \tag{4}$$

where q is the covariance of the white acceleration noise of the continuous time model. Here q is chosen to approximate the dynamics of a train with an typical maximum acceleration of $1\,\mathrm{m/s^2}$. A rule of thumb for choosing this parameter can be found e.g. in [8, p. 263].

The orientation $\mathcal{O}$ of a train can only change when the train is lifted up and turned by $180°$ or on a railway turntable which is very untypical in normal operation. Thus the orientation is assumed constant

$$\mathcal{O}_{k+1} = \mathcal{O}_k. \tag{5}$$

The combination of (3) and (5) results in the overall system model

$$\mathbf{x}_k = \underbrace{\begin{bmatrix} \mathbf{F}^{\mathrm{D}} & \mathbf{0}_{2\times1} \\ \mathbf{0}_{1\times2} & 1 \end{bmatrix}}_{\mathbf{F}} \mathbf{x}_{k-1} + \underbrace{\begin{bmatrix} \mathbf{I}_{2\times2} \\ \mathbf{0}_{1\times2} \end{bmatrix}}_{\mathbf{G}} \mathbf{n}_{k-1}. \tag{6}$$

In (6) $\mathbf{I}_{n\times m}$ and $\mathbf{0}_{n\times m}$ are n by m identity and zero matrices.

Algorithm 1: SIR Particle Filter for Along-track Localization

1: Initialize particle set $\{\mathbf{x}_0^i,\, w_0^i\}_{1:N_p}$
2: **for all** measurements **do**
3:   **for all** particles **do**
4:     $\mathbf{n}_{k-1} \sim \mathcal{N}(0, \mathbf{Q})$
5:     $\mathbf{x}_k^i = \mathbf{F}\mathbf{x}_{k-1}^i + \mathbf{G}\mathbf{n}_{k-1}$
6:     **if** $s_k^i \notin [0, L_{\mathcal{I}}]$ **then**
7:       $s_k^i = \underset{s\in[0,L_{\mathcal{I}}]}{\arg\min}\left(|s_k^i - s|\right)$
8:     **end if**
9:     $\tilde{w}_k^i = w_{k-1}^i \cdot \mathcal{N}\left(\mathbf{y}_k; \mathrm{map}(s_k^i, \mathcal{O}_k^i), \sigma_m^2 \mathbf{I}_{3\times 3}\right)$
10:   **end for**
11:   Normalize all weights $w_k^i = \tilde{w}_k^i / \sum \tilde{w}_k^i$
12:   $N_{\text{eff}} \leftarrow 1/\sum {w_k^i}^2$
13:   **if** $N_{\text{eff}} < N_{\text{T}}$ **then**
14:     Resample and assign equal weights
15:   **end if**
16: **end for**

B. Measurement Model

The measurement model relates the along-track position to the corresponding magnetic field

$$\mathbf{y}_k = \mathrm{map}(s_k, \mathcal{O}_k) + \mathbf{w}_k \tag{7}$$

where $\mathbf{w}_k$ is the sensor noise and $\mathrm{map}(\cdot,\cdot)$ is the prior created map of the magnetic field. As mentioned before, in this paper a triad of magnetometers is used and hence $\mathrm{map}(\cdot,\cdot)$ is a vector-valued function

$$\mathrm{map} : \mathbb{R} \times \{-1, +1\} \to \mathbb{R}^3, (s, \mathcal{O}) \mapsto \mathbf{m} \tag{8}$$

mapping s to the three dimensional magnetic field $\mathbf{m}$. The orientation $\mathcal{O}$ ensures that the sign of the field is adapted correctly. In the measurements model we assume that the three magnetometers have the same noise characteristics and that the noise is uncorrelated $\mathbf{w}_k \sim \mathcal{N}(\mathbf{0}, \sigma_m^2 \mathbf{I}_{3\times 3})$.

C. Filter Algorithm

The measurement model (7) contains nonlinearities introduced by the magnetic field. To handle this nonlinearities a particle filter is applied. The particle filter approximates the posterior probability density function (pdf) $p(\mathbf{x}_{0:k}|\mathbf{y}_{0:k})$ of the state history $\mathbf{x}_{0:k}$ from time step 0 to k conditioned on the whole measurement history $\mathbf{y}_{0:k}$ with a set of weighted particles $\{\mathbf{x}_{0:k}^i, w_k^i\}_{1:N_p}$, where $\mathbf{x}_{0:k}^i$ is the state vector and w_k^i the weight of the i-th particle. For a set of N_p particles the posterior pdf can be written as

$$p(\mathbf{x}_{0:k}|\mathbf{y}_{0:k}) \approx \sum_{i=1}^{N_p} w_k^i \delta_{\mathbf{x}_{0:k}^i}(\mathbf{x}_{0:k}) \tag{9}$$

with the Dirac measures $\delta_{\mathbf{x}_{0:k}^i}(\mathbf{x}_{0:k})$

$$\delta_{\mathbf{x}_{0:k}^i}(\mathbf{x}_{0:k}) = \begin{cases} 1, & \mathbf{x}_{0:k} = \mathbf{x}_{0:k}^i \\ 0, & \mathbf{x}_{0:k} \neq \mathbf{x}_{0:k}^i \end{cases} \tag{10}$$

The weighted set for each time step k is calculated sequentially with a sampling importance resampling (SIR) filter that can be found e.g. in [9]. Algorithm 1 shows the pseudocode of the SIR filter. In the initialization phase the particles are split into two subsets with the same cardinality. The first subset contains all particles with an orientation $\mathcal{O} = +1$ and the second all particle with $\mathcal{O} = -1$. After the orientation is initialized the position and speed of the particles is set. The initial positions are the same for both subsets and are placed equidistant in the interval $\pm 50\,\mathrm{m}$ around the true along-track position. The initial speed is drawn from a uniform distribution centered at the true speed $\pm 2.5\,\mathrm{m/s}$. The weights are all set to $1/N_p$.

After the filter is initialized, an iteration is performed for each measurement. A single iteration contains two steps, the prediction step (line 4–8) and the update step (line 9 and 11). In the prediction step the state of the particles at time k is calculated based on samples of the system noise and the state at $k-1$. The condition in line 6 ensures that the along-track position is always valid and within the interval $[0, L_{\mathcal{I}}]$ defined by the track. When the position is not in this interval, the position is set to the closest valid value. This is followed by the update step that adjusts the particle weights. In the context of importance sampling the weight update is [9]

$$\tilde{w}_k^i = w_{k-1}^i \frac{p(\mathbf{y}_k|\mathbf{x}_k^i) p(\mathbf{x}_k^i|\mathbf{x}_{k-1}^i)}{q(\mathbf{x}_k^i|\mathbf{x}_{k-1}^i, \mathbf{y}_k)} \tag{11}$$

where $\mathbf{q}(\cdot)$ is the importance density. In the case of the SIR filter the importance density is chosen to be the prior $p(\mathbf{x}_k^i|\mathbf{x}_{k-1}^i)$, reducing the weight update to a multiplication of the old weight with the likelihood

$$p(\mathbf{y}_k|\mathbf{x}_k^i) = \mathcal{N}\left(\mathbf{y}_k; \mathrm{map}(s_k^i, \mathcal{O}_k^i), \sigma_m^2 \mathbf{I}_{3\times 3}\right) \tag{12}$$

defined by the measurement model (7). The weights $\tilde{w}_k^i$ are only proportional to the true weights and hence have to be normalized (line 11) to ensure that the sum over all weights is one. In contrast to e.g. a Kalman filter, the update step of a particle filter has no feedback mechanism. Without further action the particle cloud will spread according to the system model (6) and the filter will diverge over time. This effect is also known as particle depletion [10]. The depletion is tackled by resampling when the effective number of particles

$$N_{\text{eff}} = \frac{1}{\sum\limits_{i=1}^{N_p} {w_k^i}^2} \tag{13}$$

falls below a threshold N_{T}. For resampling the systematic resampling algorithm, see e.g. [9], is used. In the resampling step it is assumed that the new particles are samples from the true posterior and hence equal weights are assigned to all particles.

D. Filter Output

In the evaluation of the SIR filter in respect to the localization accuracy a single estimate for the state vector is required. For this purpose the estimate minimizing the Bayesian mean square error (MMSE) [11] is calculated

$$\hat{\mathbf{x}}_{0:k} = E[\mathbf{x}_{0:k}|\mathbf{y}_{0:k}] = \int \mathbf{x}_{0:k} p(\mathbf{x}_{0:k}|\mathbf{y}_{0:k}) d\mathbf{x}_{0:k}. \tag{14}$$

By inserting (9) into (14) the MMSE estimate becomes

$$\hat{\mathbf{x}}_{0:k} \approx \int \mathbf{x}_{0:k} \sum_{i=1}^{N_p} w_k^i \delta_{\mathbf{x}_{0:k}^i}(\mathbf{x}_{0:k}) d\mathbf{x}_{0:k} = \sum_{i=1}^{N_p} w_k^i \mathbf{x}_{0:k}^i. \quad (15)$$

The MMSE estimate is therefore the weighted sum over all particles.

IV. Evaluation

The feasibility of the proposed localization system is evaluated based on a dataset recorded with a diesel train running on the track network of the Harzer Schmalspurbahnen, a regional train provider in northern Germany. In the evaluation we used the same dataset as in [3] that consists of three different tracks with a total length of roughly $13\,\mathrm{km}$ and a duration of $32\,\mathrm{min}$. The maximum speed of the diesel train during the measurements was $40\,\mathrm{km/h}$.

A. Measurement Setup

For the measurements a Xsens MTi-G-700 IMU containing also a triad of magnetometers was mounted on the floor of the train cabin. The magnetic field was recorded with $100\,\mathrm{Hz}$. The ground truth, for the map creation and for evaluating the positioning error of the magnetic field based approach, is obtained with a u-blox LEA-M8T GNSS receiver at a rate of $1\,\mathrm{Hz}$. The magnetic field map is based on a second set of measurements recorded during a different run on the same tracks. To create the map each magnetometer measurement is first stored with the corresponding along-track position obtained from the GNSS receiver. In an second step the measurements are linearly interpolated on equidistant grid with a spacing of $0.1\,\mathrm{m}$. The time difference between recording the map data and the data used for localization depends on the track and was between a couple of minutes and $32\,\mathrm{h}$. The particle filter uses 2000 particles and is updated at a rate of $10\,\mathrm{Hz}$.

B. Results

In Table I the root mean square error (RMSE) of the along-track position is shown. The error ε is the difference between the particle filter MMSE estimate $\hat{s}_k$ and the along-track position s_k from the GNSS receiver. The GNSS along-track position is obtained from an orthogonal projection of the GNSS position on the map. The RMSE is defined by the equation

$$\bar{\varepsilon} = \sqrt{\frac{1}{N}\sum_{k=1}^{N}(\hat{s}_k - s_k)^2} = \sqrt{\frac{1}{N}\sum_{k=1}^{N}\varepsilon_k^2}. \quad (16)$$

In addition to the RMSE Table I shows the maximum magnitude and the 95% and 99% quantile of the position error.

The RMSE of the proposed particle filter approach is close to the performance of a simple single frequency GNSS receiver and almost identical to the RMSE of our prior work in [3]. The approach in [3] was evaluated with the same dataset and is based on an IMU that was stabilized with position estimates obtained from the cross-correlation of the magnetic field map and the current magnetometer measurements. Even though the difference in the RMSE of the particle filter

TABLE I
RMSE $\bar{\varepsilon}$, MAXIMUM VALUE $\varepsilon_{\mathrm{MAX}}$, 95% QUANTILE q_{95} AND 99% QUANTILE q_{99} OF THE ALONG-TRACK POSITION ERROR $|\varepsilon|$

	$\bar{\varepsilon}$ [m]	q_{95} [m]	q_{99} [m]	$\varepsilon_{\max}$ [m]
Track 1	5.45	10.82	28.72	31.68
Track 2	3.68	4.07	17.46	43.48
Track 3	1.87	2.86	3.33	4.06
Overall	3.84	5.11	19.54	43.48

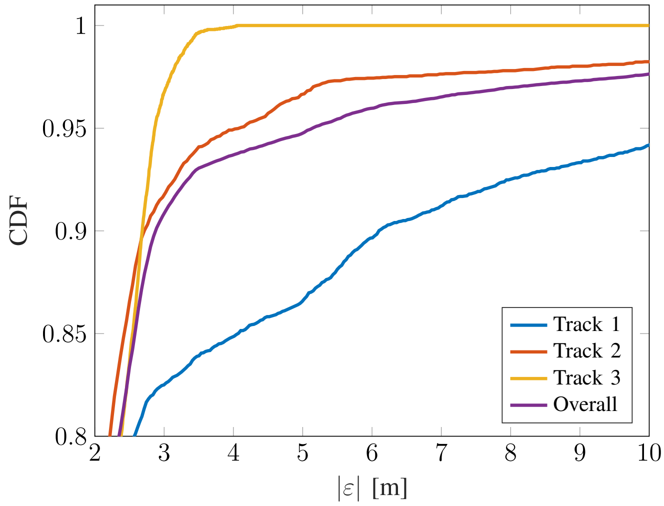

Fig. 2. CDF of the absolute along-track position error for the different tracks and the overall dataset.

and the IMU aided approach is negligible, the use of the IMU reduced the maximum position error below $20\,\mathrm{m}$. A comparison of the different tracks shows that the accuracy that can be reached strongly depends on the track and therefore on the magnetic field. If only the RMSE is considered the performance on the different tracks is comparable. A bigger difference can be seen when the quantiles and the maximum error is compared. The maximum error of Track 3 is an order of magnitude smaller then for the other tracks. The same is observed for the 99% quantiles. This can be seen also from the cumulative distribution function (CDF) in Fig. 2. The particle filter position estimate for Track 1 and 2 shows large correlated errors for a duration of multiple seconds. This results in a CDF that only slowly converges to one. The large correlated errors are due to the magnetic field on the tracks. When the magnetic field along the track has no or only small variation no information can be gained from the magnetometer measurements. For localization it is crucial that the magnetic field shows measurable variations when the position changes. When this is not the case the particles are starting to spread according to the system model and the weights of the particles are not adapted properly. In Fig. 3 the measured magnetic field, the train speed from GNSS and the along-track error of Track 2 is shown. The figure contains the $50\,\mathrm{s}$ of data when the maximum error was observed. From Fig. 3 (a) it is getting clear that magnetic field for this part of the track shows only small variations. This results in an quadratically increasing error on the position estimate Fig. 3 (c). When the magnetic field shows

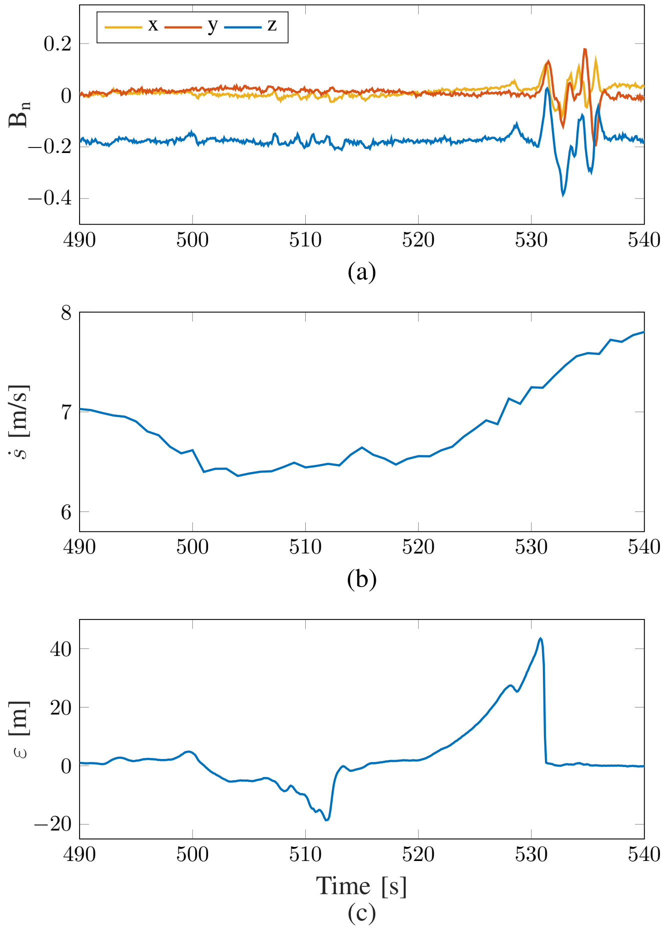

Fig. 3. (a) Measurements of the magnetometer triad. The x- and y-axis of the triad are parallel and perpendicular to the track and the z-axis is facing downwards. (b) Train speed $\dot{s}$ during the measurements. (c) Along-track estimation error of the particle filter.

only a weak dependency on the position, the error of the filter starts to become dependent on the change of the train speed. Assuming the train speed was estimated correctly before the magnetic field starts to show no variations at $490\,\mathrm{s}$, the position estimate will still be maintained for a certain time as long as the speed of the train is constant. But as can be seen in Fig. 3 (b), already small changes in the speed leads to an error growing quadratically with time. This error growth can be reduced by incorporating additional sensors that measure the train acceleration or speed. Depending on the sensor quality and type this has the potential to largely improve the position accuracy whenever the magnetic field does not exhibit strong variations. Another option to reduce the positioning errors is to manually introduce position dependent variations into the magnetic field. This could be achieved by placing permanent magnets along the track or by magnetizing the rails. The orientation was estimated properly for the different tracks. After a few filter iterations and resampling the orientation for all particles was set to the correct value. For the train speed a RMSE of $0.42\,\mathrm{m/s}$ was achieved. Comparable to the position estimate the quality of the speed estimates strongly depends on the variation of the magnetic field.

V. Conclusion

In this paper we proposed a SIR particle filter for train localization that requires only a map of the magnetic field and magnetometer measurements. The evaluation of the filter showed the feasibility of the approach and that the achievable along-track position RMSE is comparable to the error of a simple single frequency GNSS receiver. In addition to the position the orientation of the train in respect to the track was estimated correctly throughout the evaluation. This largely simplifies the filter initialization, i.e. a course train position and speed estimate is sufficient. For the speed estimate an RMSE below $0.5\,\mathrm{m/s}$ was achieved. The position and speed accuracy was mainly limited by the magnetic field that, for some short parts of the evaluated tracks, exhibits only a weak dependency on the position. This results in an error growing rapidly over time. This can be tackled easily by incorporating additional sensors like an IMU or wheel speed sensors into the particle filter prediction or update step.

Acknowledgment

Thanks goes to the Harzer Schmalspurbahnen and their staff for providing the rolling stock for the measurements.

References

[1] J. Marais, J. Beugin, and M. Berbineau, “A survey of GNSS-based research and developments for the European railway signaling,” *IEEE Transactions on Intelligent Transportation Systems*, vol. PP, no. 99, pp. 1–17, 2017.

[2] O. Heirich, B. Siebler, and E. Hedberg, “Study of train-side passive magnetic measurements with applications to train localization,” *Journal of Sensors*, Juni 2017.

[3] B. Siebler, O. Heirich, and S. Sand, “Bounding ins positioning errors with magnetic-field-signatures in railway environments,” in *Proceedings of the 30th International Technical Meeting of The Satellite Division of the Institute of Navigation (ION GNSS+ 2017)*, September 2017, pp. 3224 – 3230.

[4] M. Frassl, M. Angermann, M. Lichtenstern, P. Robertson, B. J. Julian, and M. Doniec, “Magnetic maps of indoor environments for precise localization of legged and non-legged locomotion,” in *2013 IEEE/RSJ International Conference on Intelligent Robots and Systems*, Nov 2013, pp. 913–920.

[5] J. Haverinen and A. Kemppainen, “A global self-localization technique utilizing local anomalies of the ambient magnetic field,” in *2009 IEEE International Conference on Robotics and Automation*, May 2009, pp. 3142–3147.

[6] H.-S. Kim, W. Seo, and K.-R. Baek, “Indoor Positioning System Using Magnetic Field Map Navigation and an Encoder System,” *Sensors*, vol. 17, no. 3, p. 651, Mar. 2017.

[7] J. A. Shockley and J. F. Raquet, “Navigation of ground vehicles using magnetic field variations,” *Navigation*, vol. 61, no. 4, pp. 237–252, 2014, navi.70.

[8] Y. Bar-Shalom and X.-R. Li, *Estimation and Tracking: Principles, Techniques, and Software*. Norwood: Artech House, 1993.

[9] M. S. Arulampalam, S. Maskell, N. Gordon, and T. Clapp, “A tutorial on particle filters for online nonlinear/non-gaussian bayesian tracking,” *IEEE Transactions on Signal Processing*, vol. 50, no. 2, pp. 174–188, Feb 2002.

[10] F. Gustafsson, *Statistical sensor fusion*. Lund: Studentlitteratur, 2010.

[11] S. M. Kay, *Fundamentals of statistical signal processing*. New Jersey: Prentice Hall PTR, 1993.